The Effect of Saccharin on Microstructure and Corrosion Behavior of Nanocrystalline Nickel Thin Films in Alkaline Solution

Nima Zaghian [1], Behrooz Shayegh Boroujeny [1,2,*]

[1] Advanced Materials Research Center, Department of Materials Engineering, Najafabad Branch, Islamic Azad University, Najafabad, Iran
2 Department of Materials Engineering, Shahrekord University, Shahrekord, Iran

ARTICLE INFO

Article history:

Received 21 October 2016
Accepted 22 January 2017
Available online 25 June 2017

Keywords:

Electrodeposition
Nanocrystalline Ni
Additive; Passivation
Corrosion resistance
Microstructure

ABSTRACT

In this study, the effect of crystallite size reduction and microstructure on the electrochemical corrosion behavior of nanocrystalline nickel (NC Ni) was investigated using Tafel polarization and electrochemical impedance spectroscopy (EIS) measurements in 10 wt.% NaOH. NC Ni coatings were produced by direct current electrodeposition using chloride baths in the presence and absence of saccharin as a grain refining agent. The crystallite size of NC surface coatings was calculated and analyzed by X-ray diffractometry (XRD). Field emission scanning electron microscopy (FE-SEM) and atomic force microscopy (AFM) were used to study coatings microstructure. The chemical composition of NC surfaces was determined using X-ray energy dispersive spectroscopy (EDS). Our results showed that saccharin decreased the crystallite size but increased the grain size. In addition, corrosion resistance of NC Ni in the presence of saccharin increased, which is ascribed to the formation of a more stable and protective film. The behavior of passive film growth and corrosion was also discussed.

1-Introduction

NC-materials have been the subject of intensive research in recent years because of their unique properties and applications in science and technology [1–3]. They are characterized by crystallites with a grain size less than 100 nm and high volume fraction of the grain boundary, which may comprise as much as 50% of total crystal volume [4]. Contrary to earlier expectations that the increased density of grain boundary and triple junction defects in nanostructures would have a detrimental effect on the overall corrosion performance on NC metals, extensive research over the last 15 years has shown otherwise. Grain size reduction in NC Ni [5–8], Co [9,10], Zn [11], Ni-P alloys [12–15] , Co-Ni, Fe alloys [16] or Ni-SiC composites [17] has been shown to considerably improve the corrosion performance for a wide range of electrochemical conditions. These studies have demonstrated that it is mainly due to the elimination of localized attack at grain boundaries, which, for conventional polycrystalline materials, is one of the most detrimental degradation mechanisms.

Electrodeposition has received considerable attention in recent years as a feasible and economically viable technique for producing NC coatings [18–21]. This process is a powerful method for fabrication of many highly precise products and synthesizing metallic nanomaterials with controlled shape and size [22]. Nickel is an essential engineering material

* Corresponding author:
E-mail address: b.shayegh@eng.sku.ac.ir

and electrodeposited Ni has been widely used in many fields to improve surface finishing, corrosion resistance and wear properties [23].
The NC Ni was produced by electrodeposition without the addition of any grain refining agent to the bath [5]. Additives have more of an influence on deposits properties than any other plating variables. When used at controlled, limited concentration, organic additive like saccharin refine the grain structure, provide desired tensile and ductility properties, impart leveling characteristic to the plating solution, and act as brighteners [24]. Comparisons of electrochemical corrosion of NC Ni with conventional coarse-grained Ni were studied, by several investigators. Rofagha *et al*. [5] have reported that 32 nm-grained Ni exhibited a higher passive current density in de-aerated 1 M H_2SO_4 compared with coarse-grained (100µm) polycrystalline Ni. Mishra *et al.* [25] have also investigated the electrochemical and corrosion behavior of NC Ni of different grain sizes (8-28 nm) in 1 M H_2SO_4. They reported that the passive current densities for NC Ni were higher than that for bulk Ni because of a defective nature of passive films on NC Ni, while the breakdown potential for NC Ni was higher than that for coarse-grained polycrystalline Ni. However, they reported that the corrosion rate of freshly exposed NC Ni was lower to compare with the bulk Ni, indicating a higher hindrance to anodic dissolution from the Ni surface. The higher breakdown potential of the NC Ni coatings compared to microcrystalline counterparts in 3.5% NaCl solution was reported by Raeissi *et al.* [26]. However, they observed that in the case of NC deposits, coatings with higher grain size showed higher resistance to pitting corrosion. Zhao *et al*. [27] have investigated the corrosion resistance of NC Ni with the grain size ranging from 30 to 28 nm in 3.5% NaCl solution. They did not observe the clear dependence of the corrosion resistance on the grain size; the higher corrosion resistance (R_{ct} = 42 kΩ cm^2) showed the 49 nm-grained specimen. Wang *et al*. [28] have investigated the effect of grain size reduction on electrochemical corrosion behavior of NC Ni in alkaline solution (10% NaOH). They reported that the corrosion resistance gradually increased with the grain size reduction from 3 µm to 16 nm due to the faster formation of continuous Ni hydroxide passive films at surface crystalline defects and relatively higher integrity of passive film.

Halide baths, especially chloride, have been shown to be suitable for obtaining deposits with good protection properties. The presence of chloride has two main effects: it assists anode corrosion and increase the diffusion coefficient of nickel ions thus permitting a higher limiting current density. Fine-grained nickel deposits are produced from chloride baths. There are a few studies about nickel electrodeposition from chloride baths and corrosion behavior of nickel films which are obtained from chloride baths. So, the aim of the present work is to investigate the corrosion behavior of NC Ni thin films from chloride baths by considering effect of grain size and microstructure in alkaline solution. NC Ni thin films of different grain sizes were produced by direct current electrodeposition technique onto copper substrates using a plating bath, both with saccharin and without saccharin addition. The structure of NC Ni thin films was characterized using FESEM, XRD and AFM. The chemical composition of NC surfaces was determined using EDS. Corrosion resistance was studied using polarization and electrochemical impedance spectroscopy (EIS).

2- Experimental

2-1- Specimen preparation and electroplating conditions

NC Ni coatings with different grain sizes were deposited on copper plates using nickel chloride electrolyte containing 0.1 M nickel chloride ($NiCl_2.6H_2O$), 0.5 M ammonium chloride (NH_4Cl), 0.5 M boric acid (H_3BO_3) [29]. Copper is the most commonly substrate for studies on nickel plating, primarily due to structural compatibility between copper and nickel leading to better adhesion of electrodeposits. Saccharin (0.2 M) was also added to the bath in some of electrodeposition experiments for reducing the grain size. Electrodeposition experiments were performed at room temperature (~ 25 ºC) using a current density of 0.03 A/cm^2 with direct current. A nickel sheet of 99.99% purity with dimensions of 70 mm × 30 mm × 3 mm was used as anode and pure copper plate with dimensions of 10 mm × 10 mm × 2 mm as cathode (substrate). Total time of deposition was 5 min and the thickness of coatings was 1 µm. prior to electrodeposition, the copper substrates were mechanically polished with silicon carbide papers of 400, 600, 800, 1200 grits then rinsed with distilled water. During the electroplating

process, it was found that the pH of the solution plays an important role on quality of the deposits and the pH range of 3.5 to 4.5 resulted in the deposits with bright appearances and free of voids and cracks. Hence, the pH of the bath was kept 4.0 ± 0.2 [30].

2-2- Characterization of nanocrystalline coatings

FE-SEM (MIRA TESCAN III) and AFM, in tapping mode (Olympus SiN rectangular cantilever, resonance frequency of 71 kHz, spring constant of 0.73 N/m),Film investigated areas were always of 1×1 μm^2 were used to study coatings microstructure. The chemical composition of NC surfaces was determined using EDS. Crystallite size of deposits was calculated by the (111) X–ray diffraction (XRD, Philips X´pert) peak broadening. The diffraction patterns were obtained using CuK_α (λ = 0.15406 nm) radiation over 2θ angle of 10º - 90º. The full width half maxima (FWHM) of diffraction peaks were estimated by pseudo-voigt curve fitting. The crystallite size was estimated using the Scherrer equation [31]:

$$D=0.9\lambda/\beta\cos\theta \quad (1)$$

where D is the average crystallite size, λ is the wavelength of the X-ray, θ is the Bragg angle for the peak and β is the true profile FWHM. The β parameter was calculated using Gaussian-Cauchy equation. It has been shown that the crystallite size measured by the Gaussian-Cauchy equation is similar to what is obtained by TEM observations [26]. The bulk Ni with average grain size of 80 µm was used as reference sample to determine instrumental broadening corrections. The main problem of microscopic technique is the resolution of single grain because the crystallite are often overlapped [32]. In addition, it is accepted that a crystallite size is the coherent diffraction domain in the film and that the grains are larger than crystallites and are formed by several of them [33,34]. So XRD was used for the crystallite size determination and FESEM for the grain size. The composition of electrolytes and crystallite sizes summarized in Table 1.

2-3- Electrochemical measurements

Corrosion properties of NC coatings were measured both using potentiodynamic tests and EIS analysis. Additionally, potentiodynamic analysis and EIS were carried out on a bulk Ni sample in order to compare the results with NC coatings. The electrochemical measurements were performed in a three electrode cell where sample was immersed in 10 wt. % NaOH solution and connected to potentiostat/galvanostat (Princeton Applied Research, PAR) as a working electrode. During the tests, a graphite electrode and a saturated calomel electrode (SCE) were used as counter and reference electrode. The polarization scanning was started at $0.25V_{SCE}$ blow corrosion potential to an anodic potential of $1V_{SCE}$ above corrosion potential. The scanning rate of potentiodynamic polarization measurements was 1 mV/S. Potentiodynamic anodic polarization curves were acquired and corrosion potential (E_{Corr}) and corrosion current density (i_{Corr}) were determined using the Tafel extrapolation method. The corrosion parameters were extracted from the polarization curves using commercial software CorrView. EIS is a unique and non-destructive tool for understanding the true nature of electrochemical reactions. The steps of electrochemical reactions are observed by proposing electrical circuits and calculating numerical results which are then related with the condition of the surface after reaction [35]. EIS measurements were conducted by applying an alternating sine signal to the samples with an amplitude of 10 mV. The frequency range was chosen between 100 KHz to 10 mHz. The EIS data were modelled using Zview software. Total samples which used for electrochemical measurements were 18.

Table 1. Composition and crystallite size of the baths [29].

Bath	**Concentration, M**				**Crystallite size (nm)**
	$NiCl_2$	NH_4Cl	$C_7H_4NNaO_3S$	H_3BO_3	
$NiCl_2$	0.1	0.5	-	0.5	28
$NiCl_2$ + Saccharin	0.1	0.5	0.2	0.5	10

3- Result and Discussion

3-1- Effect of saccharin on microstructure

The grain size of the bulk Ni sample was determined using optical microscopy (OM) as seen as in Fig. 1. The mean grain size of the surface was approximately 80 µm. Fig. 2 shows the XRD patterns of the bulk Ni sample and the NC Ni coatings. The diffraction peaks at 44.52º, 51.97º and 76.51º correspond to nickel crystallographic planes of (111), (200) and (220). The crystallite sizes of the NC Ni coatings varied between 28 and 10 nm. Texturing was evident in the electrodeposited nickel using saccharin in the bath. The XRD patterns indicate that there was a preferential growth in the case of NC Ni coatings with saccharin as additive and the possible role of grain refining agent in causing texturing.

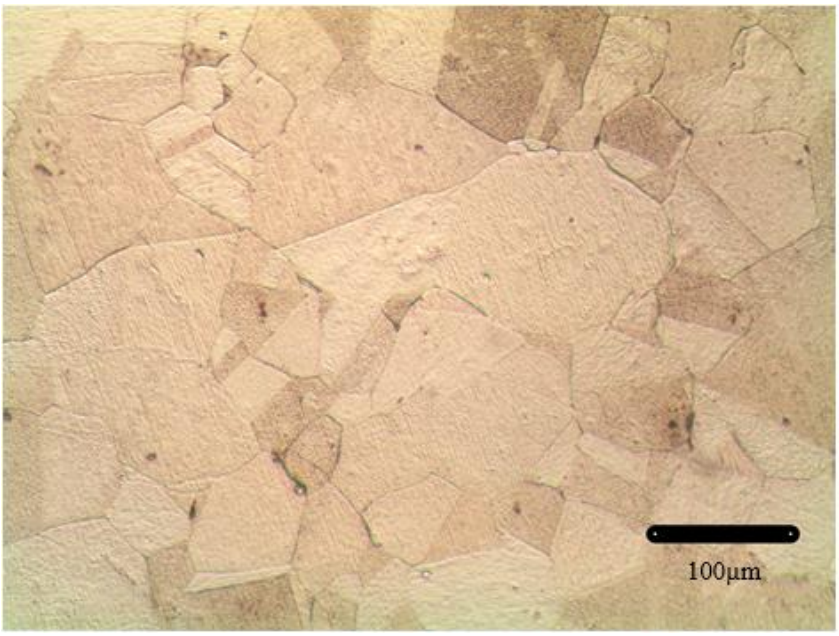

Fig. 1. Optical image of bulk Ni sample (annealed state).

It is anticipated that adsorption of saccharin on (200) and (220) planes would retard the growth of (200) and (220) planes, while facilitating the growth of (111) planes. In addition, the broadening of the diffraction peaks is observed, which can be attributed to the ultrafine crystallite size (28 and 10 nm).

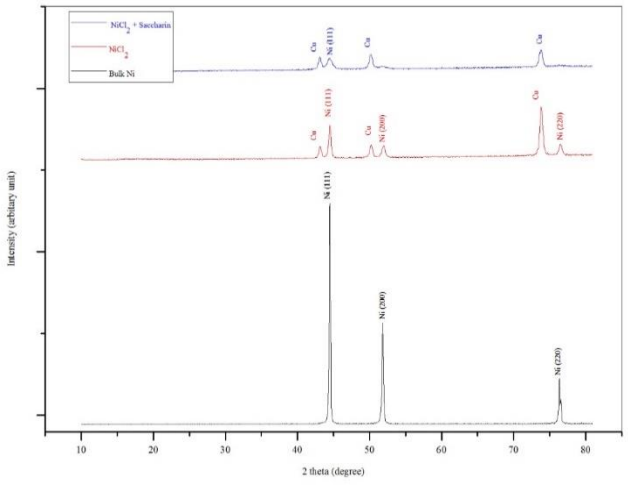

Fig. 2. XRD patterns of the samples.

In Fig. 3, microstructure of the NC Ni coatings is shown in FE-SEM micrographs in the absence and presence of saccharin in deposition bath. A dense nickel layer was obtained. In Fig. 3a, nickel has a spherical and regular nodular "cauliflower-like" structure. However, addition of saccharin has resulted in a substantial modification of microstructure of the coating as revealed in the FE-SEM micrograph (Fig. 3b). The micrograph shows spherical and more ordered grains in the presence of saccharin when compared to the micrograph obtained for the case without saccharin additive in the deposition bath. As can be seen in Fig. 3b, in the presence of saccharin the grain size has increased, whereas according to the XRD patterns the crystallite size has decreased. The effect of saccharin in the electrodeposition bath can be explained using the resonance structure of saccharin.

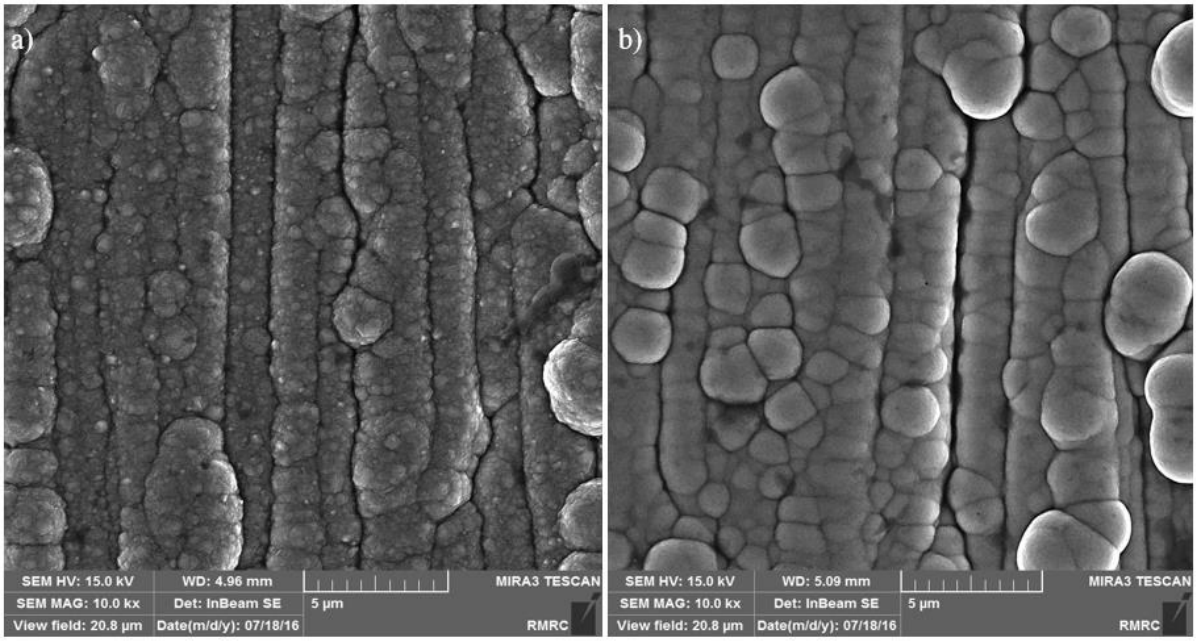

Fig. 3. FE-SEM images of Microstructure of NC Ni coatings in the absence (a) and presence (b) of saccharin.

The negative charge in the saccharide ion affects its interaction with the cathode. However, delocalization of the electron lone pair of the nitrogen atom in the N-C bond makes the N atom fractionally positive (δ^+) and the O atom fractionally negative (δ^-) (See Fig. 4). Due to this transient ionic character, saccharide ions may start competing with Ni^+ cations in the rush toward cathode. The Ni^+ ions are smaller in size compared with the saccharides. Therefore, they may move faster and deposit at a faster rate. Consequently, saccharide ions may be arriving at the substrate after a few batches of nickel ions have been deposited. Saccharide ions so adsorbed on the substrate block the active site and prevent the growth in a preferential direction (determined by the position of N and O atoms) thereby reducing the crystallite size. Furthermore, the surface diffusion of the cations is impeded by adsorbed saccharide ions [36]. Therefore, less metal cations reach the growth sites and formation of new nuclei is preferred. Due to the presence of

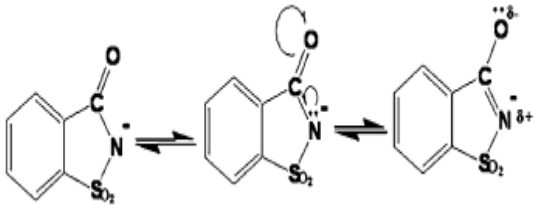

Fig. 4. Schematic representation of the delocalized of electron pair in nitrogen atom of saccharide ion over the C-N bond [32] .

fractionally negative charge on the O atom a preferable position is made on the substrate for Ni^+ ions to deposit. This makes many small crystallites at one place construct a larger grain. The Ni content in nanocrystal electrodeposited coatings was 100 atomic weight percent (at.%) measured by EDS (Fig.5). In Fig.5b, no corresponding sulfur peak was found. In fact,

the saccharide ions are the final product of saccharin oxidation on noble metal electrodes.

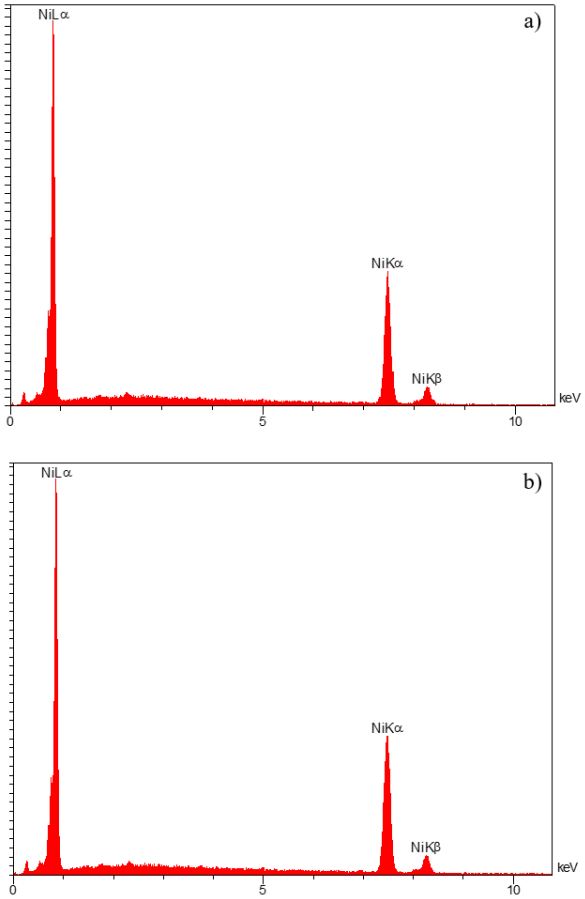

Fig. 5. EDS result of NC Ni deposits in the absence (a) and presence (b) of saccharin.

3-2- Corrosion behavior

3-2-1 Potentiodynamic polarization

Potentiodynamic polarization curves of different samples in 10 wt.% sodium hydroxide solution are shown in Fig. 6. As can be observed, by potentiodynamic polarization curves, all samples exhibit self-passivation. Active-passive behavior of metals and alloys is related to the type of electrode and electrolyte. Nickel has a great ability to form a passive film in hydroxide solution. In addition, defects like boundaries and dislocations are perfect sites for nucleation of the passive film (Forming, growing and breaking of the passive film were discussed in the passive film growth section). The corrosion parameters were extracted from the polarization curves and summarized in Table 2. It was found that the corrosion and passivation current density and corrosion potential significantly changed with the alteration of microstructural morphology and crystallite size . E_{Corr} shifted to a more positive

The saccharide ion has negative charge and it cannot be reduced.

potential in the presence of saccharin because of the change in kinetics for hydrogen evolution reaction [25]. It is known that defects like dislocation affect the kinetics of hydrogen reaction. Moreover, reversible trapping of hydrogen at dislocations, grain boundaries, and pores can change the kinetics of hydrogen evolution. Therefore, catalysis of the hydrogen reduction process by a substantial quantity of crystalline defects (e.g. grain boundaries) at the surface of NC Ni coating shifts the E_{Corr} value to positive direction [5].

The corrosion current density of NC Ni coatings was much higher than that of bulk Ni. This higher current density was attributed to the higher grain boundary and triple junction content in the NC samples, which provide sites for electrochemical activity, and this is the main reason for faster forming of the passive layer in the presence of saccharin than in the absence of saccharin. Another reason is the pores in the NC Ni coatings because in aqueous solution the cathode hydrogen evolution happens and it forms pores [37, 38]. However, this difference in current density diminishes at higher potentials (0.55 V_{SCE}) at which the overall dissolution rate overwhelms the controlled dissolution rate of the structure observed at lower potentials. The current appeared to be the anodic limiting current plateau resulted from mass transfer of dissolution product from the Ni surface to the bulk electrolyte. The polarization curve of the NC Ni coating in the absence of saccharin showed a passive, though not protective, behavior. The passivity is unstable due to the chemical dissolution of the passive film into the solution. There was a noticeable change in the passive current density for the NC Ni coatings compared to bulk Ni. The NC Ni coatings showed higher passive current density compared to bulk Ni. This indicates the defective nature of the passive film that is formed on NC Ni. Characterization of the passive film on the NC Ni coatings by X-ray photoelectron spectroscopy has shown that a larger number of defects were present in these films [28]. It has been suggested that this should be due to easier Ni cations diffusion through a more defective film, thereby leading to higher passive current densities in the passive range for the NC Ni coatings [39]. The imperfection passivation associated with NC Ni may also be

related to intrinsic electrochemical behavior associated with the disordered intercrystalline region in nickel [5, 40]. The fluctuation in anodic polarization curves before reaching a certain potential in each curve may be due to variation in the concentration of the products of anodic reaction or, in other words, it undergoes several oxidation stages during anodic polarization.

3-2-2 Passive film growth

Since the solubility of salts is limited, an excessive accumulation of metal ions in the near- electrode layer will cause the salts to precipitate out onto the electrode, screening a considerable portion of its surface and sharply increasing the current on the free part of the surface. Upon hydrolysis of sodium hydroxide, the hydroxide ions appear which are able to form a passivating film on the Ni surface. Since the migration or diffusion of cations from the metal lattice into the solution through such a passive layer is more difficult, the rate of the anodic process begins to drop. In the passive region, two electrochemical reactions were proceeding at the same time, anodic dissolution of metal through the passive film and electrochemical oxidation of the electrode by hydroxyl ions or by oxygen of water. The greater positive shift in potential, the more electric-field intensity in oxide will increase, which should also increase the velocity of motion of cations through the film. However, there is a simultaneous acceleration of the reaction of electrochemical oxidation of the metal by hydroxyl ions or oxygen, so that the thickness of the film increases as well. This makes it more difficult for the metal cations to emerge from the lattice into the electrolyte. As a result of two opposing factors, the anodic current varies slightly and remains constant with a change in the potential. By increasing the potential, the intensity of the electric field becomes extremely high and as a result of the non-uniform coating of the passive layer an intensive dissolution of metal was initiated at the breakdown potential.

The anodic potentiodynamic polarization curves (Fig. 6) show that by decreasing the crystallite size (in the presence of saccharin) the adsorption of OH^- ions increases and the passivation current was seen to decrease [41]. It was thought that passivation of electrode involves water molecules which are absorbed on the electrode surface according to the following mechanism including chemical and electrochemical steps [42, 43]:

$Ni + H_2O \rightarrow Ni(H_2O)_{ads}$	Chemical	(2)
$Ni(H_2O)_{ads} \rightarrow Ni(OH)^+ + H^+ + 2e^-$	Electrochemical	(3)
$Ni(OH)^+ + OH^- \rightarrow Ni(OH)_2$	Chemical	(4)

3-2-3 Electrochemical impedance spectroscopy

In order to investigate the effect of crystallite size reduction and microstructure on the stability of the passive film, impedance measurements were also carried out. The impedance spectrum diagram obtained for the frequency range of100 kHz to 10 mHz at the open circuit potential in 10 wt.% sodium hydroxide solution at 25 °C is shown in Fig. 7. The Nyquist plots reveal capacitive arcs from high to low frequencies, which are characterized by single semicircles, suggesting the involvement of single time constant.

To account for the corrosion behavior of NC Ni coatings and bulk Ni in NaOH solution, an equivalent circuit model (Fig. 8) has been proposed to simulate the metal/solution interface. In this model, R_S and R_{ct} represent the solution and charge transfer resistance, respectively, and CPE is the capacitance of the passive film represented by the constant phase element. The main reasons for using CPE are, capacitor in EIS often does not behave ideally due to the complicated corrosion process at the interface and in the presence of a fully capacitive and protective passive film [44, 45]. On the other hand,

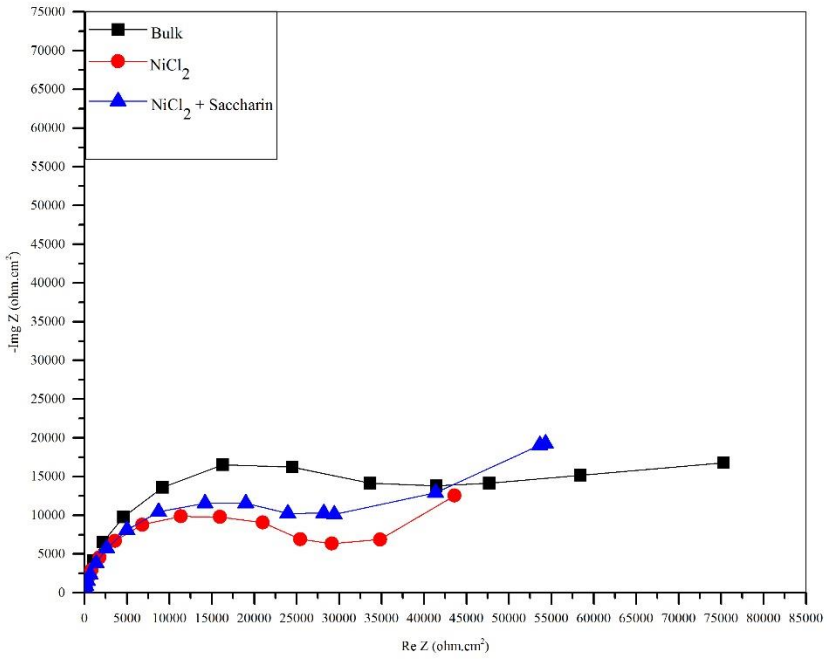

Fig.7. Nyquist plots of the samples.

CPE is generally used as a substitute for an ideal capacitor for representing samples which have rough surfaces and phase values below 90° [46, 47]. The impedance of CPE is defined as [48]:

$$Z_{CPE} = [Q (j\omega)^n]^{-1} \quad (5)$$

where n is the exponent of CPE ranging from -1 to 1, jω is the complex variable for sinusoidal perturbations with ω = 2πf, and Q is the capacitance value of the passive film. In addition, a diffusion-controlled charge transfer (Z_w) was observed at low frequencies. Such a diffusion process may indicate that the corrosion mechanism is controlled not only by a charge transfer step but also by the diffusion process. The fitted parameters of the equivalent circuit are given in Table 3.

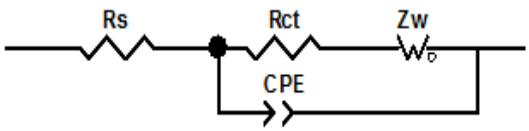

Fig. 8. Equivalent electrical circuit models used for fitting the Nyquist diagrams

It can be seen that the R_S values are similar in respective tested solutions, because the position of the working electrode and the reference electrode are fixed during the test. A higher R_{ct} was obtained for bulk nickel compared with the NC Ni coatings. This implies that bulk nickel was more resistant to anodic dissolution. This is an interesting result because it indicates that the surface of NC Ni coatings is more prone to corrosion than bulk nickel. As shown in Table 3, the values of n are close to 1, indicating that the passive films formed on all of the samples are near ideal capacitors with a compact structure. In the case of NC Ni coatings, capacitance of the passive film decreases with the reduction of crystallite size, indicating the smooth and protective nature of NC Ni coatings. On the other hand, the capacitance Q is related to the nature of a passive film and can be expressed as follows [49]:

$$Q = \varepsilon\varepsilon_0 A / L \quad (6)$$

where ε is the dielectric constant of passive film, ε_0 is the dielectric constant of free space, A is the surface area of working electrode, and L is the thickness of the passive film. A high value of capacitance corresponds to a small thickness of a passive film.

Table 3. Calculated results for EIS analysis by fitting the equivalent electrical circuit given in Fig. 8.

Sample	R_S (ohm.cm^2)	R_{ct} (kohm.cm^2)	Q (μF.cm^{-2})	n
Bulk Ni	8.17 ± 0.02	39.41 ± 0.02	6.86 ± 0.02	0.92
$NiCl_2$	6.15 ± 0.02	24.66 ± 0.02	9.06 ± 0.02	0.91
$NiCl_2$ + Saccharin	6.36 ± 0.02	29.60 ± 0.02	3.45 ± 0.02	0.90

Based on the fitted Q values listed in Table 3, it can be deduced that the passive films formed on bulk Ni and NC Ni coating in the presence of saccharin are thicker than that on NC Ni coating in the absence of saccharin. Since the passive film formed on a metal can act as a barrier in the corrosion process [11], a thicker and compact passive film would be more beneficial to prevent the metal from corrosion. According to Table 2, in the presence of saccharin i_{corr} has increased. However, Table 3 shows that in the presence of saccharin R_{ct} has increased, because addition of saccharin reduces the crystallite sizes and increases the boundaries, so i_{corr} has increased but as we can see in Fig. 6, it helps the faster formation of the passive film.

The corrosion resistance of the NC Ni coating in the presence of saccharin is improved by rapid formation of the passive film on the surface crystalline defects. Compared to the NC Ni coating, in the absence of saccharin, a relatively higher integrity of passive film is formed on nanocrystal electrodeposited Ni in the presence of saccharin. This result contradicts with the classic corrosion theory that nanostructured should accelerate corrosion by forming many more micro-electrochemical cells between the huge amount of grain boundaries and the matrix. In addition, the passivation first started on the crystalline lattice defects and nanocrystal materials has a high density of grain boundaries and dislocations inside grains [50]. Also, the nanostructure coating contains an appreciable volume fraction of interphase or grain boundaries and correspondingly large specific interphase energy [41]. Hence, it is believed that the nanocrystal electrodeposited Ni in the presence of saccharin has a high density of nucleation sites for the passive film, which leads to a high fraction of the passive layer. Fig. 9 shows AFM images of the NC Ni coatings in the presence and absence of saccharin. Average surface roughness (R_a) in the absence of saccharin was 0.020 μm and in the presence of saccharin was 0.011 μm. According to Fig. 9, the surface structure in the presence of saccharin is completely different. Saccharin inhibits the columnar growth and makes surface smoother. It is known that electrodeposits with columnar structure exhibit a higher rate of transport of material between the external surface and the electrodeposit/substrate interface [51]. This allows for easier access of the corrosive species to the coating/substrate interface. So, the corrosion resistance of the NC Ni coating in the presence of saccharin is higher. In addition, the smoother surface offers a better corrosion resistance and vice versa. Smoother surface decreases the possibility of forming metastable pits. In addition, the passive film formation on the corroded surface is diffusion controlled and the diffusion of elements in the NC Ni coating in the presence of saccharin is much higher than NC Ni coating in the absence of saccharin.

4- Conclusion

In this study, corrosion behavior of NC Ni thin films in 10 wt.% sodium hydroxide wasinvestigated. The NC deposits were obtained by direct electrodeposition using chloride bath in the presence and absence of saccharin as the grain refining agent. Texturing was observed in the case of NC Ni with saccharin as additive. In the presence of saccharin, crystallite size decreased but the grain size increased because of the resonance structure of saccharin. Morphology changed from regular nodular "cauliflower-like" to spherical by addition of saccharin. The corrosion behavior of NC Ni thin films was compared to bulk Ni. All samples exhibited an active-passive behavior. The corrosion potential shifted to noble direction with decreasing the crystallite size has been related to modification in cathodic reaction (hydrogen reduction) processes. The passive current densities for NC Ni were higher than that bulk and this has been related to the defective nature of the passive film on NC Ni. According to the EIS analysis,

the corrosion resistance for NC Ni was lower compared to bulk Ni. The porous nature of NC deposits has been related to their lower resistance. The corrosion resistance of NC Ni in the presence of saccharin was higher than NC Ni in the absence of saccharin because of faster forming and smoother passive film.

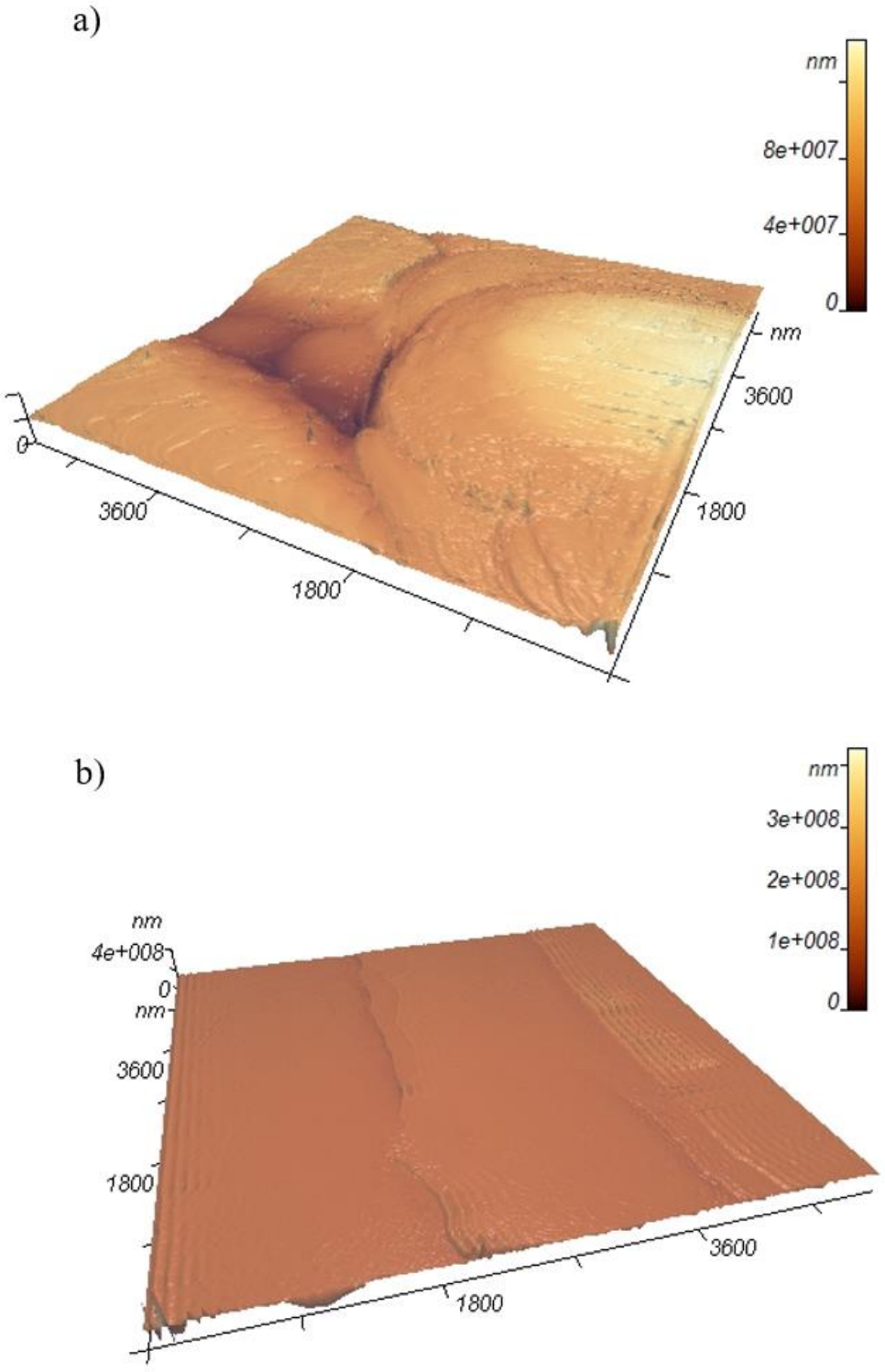

Fig. 9. AFM images of NC Ni coatings in the absence (a) and presence (b) of saccharin.

References

[1] Z. Bou-Saleh, S. Omanovic, "Nickel-Based 3D Electrocatalyst Layers for Production of Hydrogen by Water Electrolysis in an Acidic Medium", J. Nanosci. Nanotechnol., Vol. 9, 2009, pp. 2469–2479.

[2] A. Chami, B. Nasiri-tabrizi, "Effect of Heating Rate on Morphological Features of Oxidized Electroless Nickel – Boron Coatings", Vol. 3, 2015, pp. 61–70.

[3] R.. Valiev, R.. Islamgaliev, I.. Alexandrov, "Bulk nanostructured materials from severe plastic deformation", Prog. Mater. Sci., Vol. 45, 2000, pp. 103–189.

[4] H. Gleiter, "Nanostructured materials: basic concepts and microstructure", Acta Mater., Vol. 48, 2000, pp. 1–29.

[5] R. Rofagha, R. Langer, A.M. El-Sherik, U. Erb, G. Palumbo, K.T. Aust, "The corrosion behaviour of nanocrystalline nickel", Scr. Metall. Mater., Vol. 25, 1991, 2867–2872.

[6] S. Wang, Electrochemical Properties of Nanocrystalline Nickel and Nickel-Molybdenum Alloys, Ph.D. Thesis, University of Queen, Ontario, 1998.

[7] P.T. Tang, T. Watanabet, J.E.T. Andersen, G. Bech-Nielsen, "Improved corrosion resistance of pulse plated nickel through crystallisation control", J. Appl. Electrochem., Vol. 25, 1995, pp. 347–352.

[8] S.H. Kim, U. Erb, K.T. Aust, F. Gonzalez, G. Palumbo, "The corrosion behavior of nanocrystalline electrodeposits, Plat", Surf. Finish., Vol. 91, 2004, pp. 68–70.

[9] S.H. Kim, K.T. Aust, U. Erb, F. Gonzalez, G. Palumbo, "A comparison of the corrosion behaviour of polycrystalline and nanocrystalline cobalt", Scr. Mater., Vol. 48, 2003, pp. 1379–1384.

[10] A. Aledresse, A. Alfantazi, "A study on the corrosion behavior of nanostructured electrodeposited cobalt", J. Mater. Sci., Vol. 39, 2004, pp. 1523–1526.

[11] K.M.S. Youssef, C.C. Koch, P.S. Fedkiw, "Improved corrosion behavior of nanocrystalline zinc produced by pulse-current electrodeposition", Corros. Sci., Vol. 46, 2004, pp. 51–64.

[12] R. Rofagha, U. Erb, D. Ostrander, G. Palumbo, K.T. Aust, "The effects of grain size and phosphorus on the corrosion of nanocrystalline Ni-P alloys", Nanostructured Mater., Vol. 2, 1993, pp. 1–10.

[13] S.J. Splinter, R. Rofagha, N.S. McIntyre, U. Erb," XPS Characterization of the Corrosion Films Formed on Nanocrystalline Ni-P Alloys in Sulphuric Acid", Surf. Interface Anal., Vol. 24, 1996, pp. 181–186.

[14] F. Gonzalez, A.M. Brennenstuhl, G. Palumbo, U. Erb, P.C. Lichtenberger, "Electrodeposited Nanostructured Nickel for In-Situ Nuclear Steam Generator Repair", Mater. Sci. Forum., Vol. 225–227, 1996, pp. 831–836.

[15] G. Palumbo, F. Gonzalez, a. M. Brennenstuhl, U. Erb, W. Shmayda, P.C. Lichtenberger, "In-situ nuclear steam generator repair using electrodeposited nanocrystalline nickel", Nanostructured Mater., Vol. 9, 1997, pp. 737–746.

[16] M. Saito, K. Yamada, K. Ohashi, Y. Yasue, Y. Sogawa, T. Osaka, "Corrosion Properties of Electroplated CoNiFe Films", J. Electrochem. Soc., Vol. 146, 1999, pp. 2845-2848.

[17] L. Benea, P. Luigi, A. Borello, S. Martelli, "Wear corrosion properties of nano-structured SiC – nickel composite coatings obtained by electroplating", Wear., Vol. 249, 2002, pp. 995–1003.

[18] A.M. Rashidi, A. Amadeh, "The effect of saccharin addition and bath temperature on the grain size of nanocrystalline nickel coatings", Surf. Coatings Technol., Vol. 204, 2009, pp. 353–358.

[19] S.C. Tjong, H. Chen, Nanocrystalline materials and coatings, SP-88, Department of Physics and Materials Science, Hong Kong, Hong Kong, 2004.

[20] L. Wang, Y. Gao, T. Xu, Q. Xue, "A comparative study on the tribological behavior of nanocrystalline nickel and cobalt coatings correlated with grain size and phase structure", Mater. Chem. Phys., Vol. 99, 2006, pp. 96–103.

[21] F. Ebrahimi, Z. Ahmed, "The effect of current density on properties of electrodeposited nanocrystalline nickel", J. Appl. Electrochem., Vol. 33, 2003, pp. 733–739.

[22] D. Bera, S.C. Kuiry, S. Seal, "Synthesis of nanostructured materials using template-assisted electrodeposition", Jom., Vol. 56, 2004, pp. 49–53.

[23] S. Khorsand, K. Raeissi, F. Ashrafizadeh, "Corrosion resistance and long-term durability of super-hydrophobic nickel film prepared by electrodeposition process", Appl. Surf. Sci., Vol. 305, 2014, pp. 498–505.

[24] M. Abraham, P. Holdway, M. Thuvander, A. Cerezo, G.D.W. Smith,

"Thermal stability of electrodeposited nanocrystalline nickel", Surf. Eng., Vol. 18, 2002, pp. 151–156.

[25] R. Mishra, R. Balasubramaniam, "Effect of nanocrystalline grain size on the electrochemical and corrosion behavior of nickel", Corros. Sci., Vol. 46, 2004, pp. 3019–3029.

[26] M.R. Zamanzad-Ghavidel, K. Raeissi, A. Saatchi, "The effect of surface morphology on pitting corrosion resistance of Ni nanocrystalline coatings", Mater. Lett., Vol. 63, 2009, pp. 1807–1809.

[27] H. Zhao, L. Liu, J. Zhu, Y. Tang, W. Hu, "Microstructure and corrosion behavior of electrodeposited nickel prepared from a sulphamate bath", Mater. Lett., Vol. 61, 2007, pp. 1605–1608.

[28] L. Wang, J. Zhang, Y. Gao, Q. Xue, L. Hu, T. Xu, "Grain size effect in corrosion behavior of electrodeposited nanocrystalline Ni coatings in alkaline solution", Scr. Mater., Vol. 55, 2006, pp. 657–660.

[29] E. Rudnik, M. Wojnicki, W. Grzegorz, "Effect of gluconate addition on the electrodeposition of nickel from acidic baths", Surf. Coatings Technol., Vol. 207, 2012, pp. 375–388.

[30] A.M. Rashidi, A. Amadeh, "Effect of electroplating parameters on microstructure of nanocrystalline nickel coatings", J. Mater. Sci. Technol., Vol. 26, 2010, pp. 82–86.

[31] B.D. Cullity, Elements of X-ray Diffraction, 2sd ed., Addison-Wesley, Reading, 1978, pp. 281–285.

[32] A.C. Mishra, A.K. Thakur, V. Srinivas, "Effect of deposition parameters on microstructure of electrodeposited nickel thin films," J. Mater. Sci., Vol. 44, 2009, pp. 3520–3527.

[33] J.R. Ares, A. Pascual, I.J. Ferrer, C. Sánchez, "Grain and crystallite size in polycrystalline pyrite thin films", Thin Solid Films., Vol. 480–481, 2005, pp. 477–481.

[34] M.L. Calzada, I. Bretos, R. Jiménez, J. Ricote, J. Mendiola, "X-ray characterisation of chemical solution deposited PbTiO3 films with high Ca doping", Thin Solid Films. Vol. 450, 2004, pp. 211–215.

[35] D.A. Harrington, P. Van Den Driessche, "Mechanism and equivalent circuits in electrochemical impedance spectroscopy", Electrochim. Acta., Vol, 56, 2011, pp. 8005–8013.

[36] H. Natter, M. Schmelzer, R. Hempelmann, H. Gleiter, C.G. Granqvist, H. Gleiter, C.C. Koch, Y.S. Cho, G.W. Nieman, J.R. Weertman, R.W. Siegel, L.E. McCandlish, B.H. Kear, B.K. Kim, R. Rofagha, R. Langer, A.M. El-Sherik, U. Erb, G. Palumbo, K.T. Aust, G. Palumbo, F. Gonzalez, A.M. Brennenstuhl, U. Erb, W. Shmayda, P.C. Lichtenberger, B. Rösing, H. Natter, "Nanocrystalline nickel and nickel-copper alloys: Synthesis, characterization, and thermal stability", J. Mater. Res., Vol. 13, 1998, pp. 1186–1197.

[37] H. Dahms, I.M. Croll, "The Anomalous Codeposition of Iron-Nickel Alloys", J. Electrochem. Soc., Vol, 112, 1965, pp. 771-775.

[38] Y.-L. Zhu, Y. Katayama, T. Miura, "Effects of coumarin and saccharin on electrodeposition of Ni from a hydrophobic ionic liquid", Electrochim. Acta., Vol. 123, 2014, pp. 303–308.

[39] R. Rofagha, S.J. Splinter, U. Erb, N.S. Mcintyre, "Xps characterization", Vol. 4, 1994, pp. 69–78.

[40] G. Palumbo, K.T. Aust, "Triple-line corrosion in high purity nickel", Mater. Sci. Eng. A., Vol. 113, 1989, pp. 139–147.

[41] V. Afshari, C. Dehghanian, "Effects of grain size on the electrochemical corrosion behaviour of electrodeposited nanocrystalline Fe coatings in alkaline solution", Corros. Sci., Vol. 51, 2009, pp. 1844–1849.

[42] W.A. Badawy, K.M. Ismail, A.M. Fathi, "Effect of Ni content on the corrosion behavior of Cu-Ni alloys in neutral chloride solutions", Electrochim. Acta., Vol. 50, 2005, pp. 3603–3608.

[43] W. a Badawy, "Electrochemical behaviour of cobalt in aqueous solutions of different pH", Jounal Appl. Electrochem., Vol. 30, 2000, pp. 693–704.

[44] M. Danışman, "The corrosion behavior of nanocrystalline nickel based thin films", Mater. Chem. Phys., Vol. 171, 2016, pp. 276–280.

[45] D. Mareci, D. Sutiman, A. Cailean, G. Bolat, "Electrochemical determination of the corrosion resistance of NiCr dental casting alloys," Prot. Met. Phys. Chem. Surfaces., Vol. 47, 2011, pp. 108–116.

[46] A. Bai, P.Y. Chuang, C.C. Hu, "The corrosion behavior of Ni-P deposits with high phosphorous contents in brine media", Mater. Chem. Phys., Vol. 82, 2003, pp. 93–100.

[47] S. Zelinka, L. Ortiz-Candelaria, "Electrochemical impedance spectroscopy (EIS) as a tool for measuring corrosion of polymer-coated fasteners used in treated wood", For. Prod., Vol. 59, 2009, pp. 77–82.

[48] D. Sachdeva, N. Gupta, R. Balasubramaniam, "Electrochemical characterisation of nanocrystalline nickel", Def. Sci. J., Vol. 58, 2008, pp. 525–530.

[49] .M. Li, C. Cai, L.X. Song, J.F. Li, Z. Zhang, M.Z. Xue, Y.G. Liu, "Electrodeposition and characterization of nano-structured black nickel thin films", Trans. Nonferrous Met. Soc. China, Vol. 23, 2013, pp. 2300–2306.

[50] A. Balyanov, J. Kutnyakova, N.A. Amirkhanova, V. V. Stolyarov, R.Z. Valiev, X.Z. Liao, Y.H. Zhao, Y.B. Jiang, H.F. Xu, T.C. Lowe, Y.T. Zhu, "Corrosion resistance of ultra fine-grained Ti", Scr. Mater., Vol. 51, 2004, pp. 225–229.

[51] M. Troyon, L. Wang, "Influence of saccharin on the structure and corrosion resistance of electrodeposited Cu/Ni multilayers", Appl. Surf. Sci., Vol. 103, 1996, pp. 517–523.